Evaluation of a Potential Generator-Produced PET Tracer for Cerebral Perfusion Imaging: Single-Pass Cerebral Extraction Measurements and Imaging with Radiolabeled Cu-PTSM

Carla J. Mathias, Michael J. Welch, Marcus E. Raichle, Mark A. Mintun, Lennis L. Lich, Andrea H. McGuire, Kurt R. Zinn, Elizabeth K. John, and Mark A. Green

Department of Radiology, Washington University School of Medicine, St. Louis, Missouri; MURR University of Missouri, Columbia, Missouri; and School of Pharmacy, Purdue University, West Lafayette, Indiana

Copper(II) pyruvaldehyde bis(N^4-methylthiosemicarbazone) (Cu-PTSM), copper(II) pyruvaldehyde bis(N^4-dimethylthiosemicarbazone) (Cu-$PTSM_2$), and copper(II) ethylglyoxal bis(N^4-methylthiosemicarbazone) (Cu-ETSM), have been proposed as PET tracers for cerebral blood flow (CBF) when labeled with generator-produced ^{62}Cu ($t_{½}$ = 9.7 min) (*1*). To evaluate the potential of Cu-PTSM for CBF PET studies, baboon single-pass cerebral extraction measurements and PET imaging were carried out with the use of ^{67}Cu ($t_{½}$ = 2.6 days) and ^{64}Cu ($t_{½}$ = 12.7 hr), respectively (*1*). All three chelates were extracted into the brain with high efficiency. There was some clearance of all chelates in the 10–50-sec time frame and Cu-$PTSM_2$ continued to clear. Cu-PTSM and Cu-ETSM have high residual brain activity. PET imaging of baboon brain was carried out with the use of [^{64}Cu]-Cu-PTSM. For comparison with the ^{64}Cu brain image, a CBF (^{15}O-labeled water) image (40 sec) was first obtained. Qualitatively, the $H_2{}^{15}O$ and [^{64}Cu]-Cu-PTSM images were very similar; for example, a comparison of gray to white matter uptake resulted in ratios of 2.42 for $H_2{}^{15}O$ and 2.67 for Cu-PTSM. No redistribution of ^{64}Cu was observed in 2 hr of imaging, as was predicted from the single-pass study results. Quantitative determination of blood flow using Cu-PTSM showed good agreement with blood flow determined with $H_2{}^{15}O$. This data suggests that [^{62}Cu]-Cu-PTSM may be a useful generator-produced radiopharmaceutical for blood flow studies with PET.

J Nucl Med 1990; 31:351–359

Generator-produced radiopharmaceuticals for positron emission tomography (PET) have long been desirable and would be particularly advantageous in establishing satellite PET imaging centers (*1–3*). Copper-62 (^{62}Cu) is the daughter radionuclide obtainable from a $^{62}Zn/^{62}Cu$ generator (*4–6*). This generator-produced positron-emitting copper radionuclide has the short physical half-life desired in a PET perfusion tracer, yet is sufficiently long-lived to allow its chemical incorporation into a variety of different compounds. If suitable copper-labeled radiopharmaceuticals were developed, generator-produced ^{62}Cu might allow the operation of clinical PET imaging centers remote from a cyclotron facility. The principle disadvantage of the $^{62}Zn/^{62}Cu$ generator system is the rather short (9.13 hr) parent half-life (*1*); this would necessitate generator replacement at 1–2-day intervals (*4*). However, this problem is somewhat offset by large production yields, of ^{62}Zn from a medium-energy cyclotron (*4,7*). Thus, there are currently numerous cyclotron/PET facilities that could act as regional distribution centers. Furthermore, a target design that combines ^{62}Zn production as a by-product from ^{123}I production has been described (*8*).

The copper(II) complex of pyruvaldehyde bis(N^4-methylthiosemicarbazone), Cu-PTSM, has been proposed as a tracer for cerebral and myocardial perfusion when labeled with ^{62}Cu (*9,10*). In this study, we evaluated [^{64,67}Cu]-Cu-PTSM and two related copper(II) bis(thiosemicarbazone) complexes, copper(II) pyruvaldehyde bis(N^4-dimethylthiosemicarbazone) (Cu-$PTSM_2$) and copper(II) ethylglyoxal bis(N^4-methylthiosemicarbazone) (Cu-ETSM) (Fig. 1). The three copper-67-labeled copper(II) bis(thiosemicarbazone) complexes studied, Cu-PTSM, Cu-$PTSM_2$, and Cu-ETSM, have previously been shown to efficiently penetrate the blood brain barrier (BBB) (*9–11*). With all three compounds, ~3% of the injected dose was found in the brain one minute after i.v. injection into rats (*9–11*). Single-pass brain extraction and radiotracer clearance of the copper complexes has now been measured in a

Received Aug. 10, 1989; revision accepted Oct. 16, 1989.
For reprints contact: Carla J. Mathias, Washington University, The Edward Mallinckrodt Institution of Radiology, 510 S. Kingshighway, St. Louis, MO 63110.

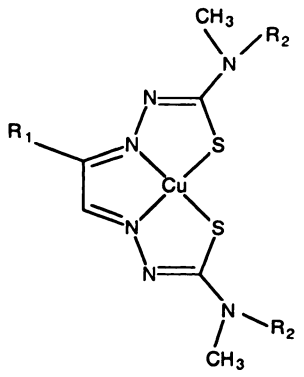

	R_1	R_2
PTSM	CH_3	H
$PTSM_2$	CH_3	CH_3
ETSM	CH_2CH_3	H

FIGURE 1
Structure of the Cu(II)bis-(thiosemicarbazone) complexes studied.

nonhuman primate (baboon) model (*12–15*), where radioactivity was detected externally by a NaI(Tl) scintillation detector after an intracarotid bolus injection. Quantitative delivery of the injected tracer to the brain is ensured in this model by prior ligation of the right external carotid artery. Cerebral imaging with [^{64}Cu]-Cu-PTSM and with PET was also carried out in baboons and these data were compared with regional cerebral blood flow (RCBF) measurements obtained with $H_2{}^{15}O$.

MATERIALS AND METHODS

The copper bis(thiosemicarbazone) complexes were prepared as described previously (*9–11*). Copper-67 was obtained as copper(II) in a 2-*M* HCl solution with a specific activity of ca. 500 Ci/mmol (Oak Ridge Isotopes Sales, Oak Ridge, TN).

Copper-64 (19% β^+) was produced via a fast neutron reaction on a high purity 99.9999% zinc metal target in a cadmium-shielded container. The ^{64}Zn(n,p)^{64}Cu reaction requires neutrons of energy >2 MeV (*16*) and was possible in the flux trap (position 18–20) of the University of Missouri Research Reactor. [The fast neutron flux averaged 9.57 (±0.27) × 10^{13}n·cm^{-2}·sec^{-1}.] Following the one-week irradiation, the zinc was dissolved in concentrated HCl, and applied to an anion exchange column (1.1 cm × 20 cm packed with either Mallinckrodt Amberlite CG-400 or Biorad AG 1-X8) pre-equilibrated with concentrated HCl (*17,18*). The ^{64}Cu was eluted with 0.6 *M* HCl, while the zinc radioactivities remained on the column. The radionuclidic purity was very high, as determined by high-resolution gamma-ray spectroscopy; the maximum levels of ^{65}Zn and ^{67}Cu detected were 0.027 and 1.78 nCi/μCi ^{64}Cu, respectively (at end of irradiation). Aliquots of the ^{64}Cu were allowed to decay, and analyzed for total copper by graphite furnace atomic absorption. The amount of copper was found to be 12.0 ± 4.4 ng/mCi of activity (at end of irradiation). This is equivalent to a specific activity ca. 5,300 Ci/mmol.

Quality control of the final radioactive copper(II) bis(thiosemicarbazone) complexes included thin-layer chromatography (TLC) on silica gel plates eluted with ethyl acetate and verification of product lipophilicity by measurement of octanol/saline (pH 6–7) partition coefficients. Radiochromatograms were analyzed on a Berthold Linear Analyzer LB282 Tracemaster 20. For animal studies, the ^{67}Cu-labeled-bis(thiosemicarbazone) complexes were injected in 0.7 ml acetate buffer solution (0.1 *M*, pH 5.5–6.5) containing ~5% ethanol. The [^{64}Cu]-Cu-PTSM was also prepared in a 5% ethanol/acetate buffer solution. All solutions were filtered through a 0.2-μm fluoropolymer filter (13 mm diameter, Gelman Acro LC13,) before injection. Production of ^{15}O-labeled-water was as described previously (*19,20*); the administered dose for the single-pass extraction experiments was ~2 mCi (0.7 ml) and for PET imaging experiments was ~30 mCi (5 ml).

The Baboon Single-Probe Model. This model, used for measuring single-pass cerebral extraction, has been described previously (*12–15,20,21*). Briefly, the method involves acquisition of time-activity curves of the brain levels of tracer after the bolus (0.2 ml) intracarotid (right) injection in adult male baboons (27–35 kg) in which right external carotid arteries were ligated at least 1 mo prior to ensure delivery into the cerebral circulation from the common carotid artery. The baboon was immobilized with 10 mg/kg ketamine i.m., and anesthesia was maintained by ventilation with 70% nitrous oxide and with 30% oxygen after paralysis was induced with galamine 2–4 mg/kg i.v. Arterial blood gases (pH, pCO_2, pO_2), end-tidal pCO_2, and arterial blood pressure were monitored. The animals are anticoagulated with 2000 units of heparin at the beginning of the experiment to prevent clotting in the catheter system used for injection. One to four increasing dose (100–1500 μCi) injections of ^{67}Cu-labeled complex were made in each animal (4 total) on each experimental occasion (8 separate experiments). Oxygen-15-labeled-water was injected in order to measure CBF (*20,21*) within 10 min of each ^{67}Cu injection; additionally, several CBF determinations were carried out at the onset of each experiment to measure the CBF and determine its stability in the animal. A final $H_2{}^{15}O$ CBF measurement was made following the last ^{67}Cu injection of the study. At least 3 wk were allowed to lapse before this experimental protocol was repeated in the same animal.

The index method for calculating the extraction (E), the CBF, and the permeability-surface area product (PS) with the external probe system has been described (*12–15*). Briefly, the system creates a time-activity curve as shown in Figure 2; also identified is the time at which the peak of the radioactivity is detected (C), as well as, 15 sec and 75 sec after peak (x and y, respectively). E can be determined from a line fitted to the tail of a 30-sec plot and extrapolated back to t = 0. The intercepts at C are measured, so that:

$$E = \frac{B_c}{A_c}.$$

To determine CBF with $H_2{}^{15}O$, x and y are measured on a 120-sec plot, as well as E calculated from a 30-sec plot:

$$I = \frac{\ln(x/y)}{E}$$

and

$$\text{CBF (mL·min}^{-1}\text{·100 g}^{-1}\text{)} = (I \times 76) + 1.3.$$

The PS for each compound can then be calculated by solving

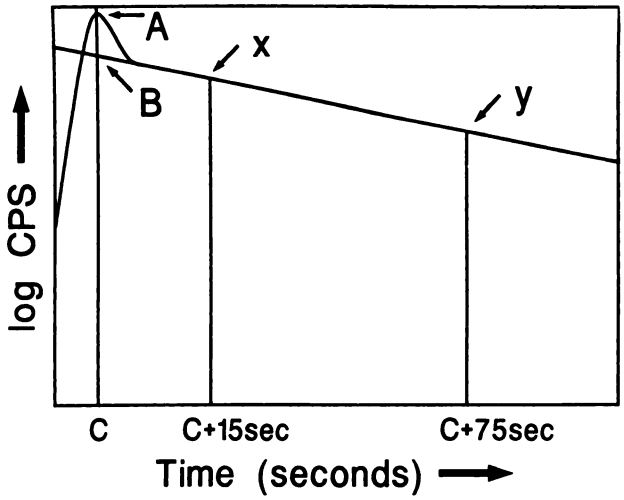

FIGURE 2
Schematic representation of a $H_2{}^{15}O$ time-activity curve from a primate brain following bolus intracarotid injection. The values of A, B, x and y are used in the index method to determine cerebral blood flow. Additionally, the brain extraction of test compounds is determined by measuring A and B at time = C. From this, the PS can be calculated.

the equation:

$$E = 1 - e^{(-PS/F)},$$

where E is the measured extraction of the compound; F is the CBF determined with $H_2{}^{15}O$; P is the capillary permeability, and S is the capillary surface area (*22–24*).

Brain Imaging Studies with [^{64}Cu]-Cu-PTSM and PET. The studies were carried out with three adult baboons anesthetized and paralyzed as described for the single-pass studies. An 18-g teflon catheter (Quickcath, 8.7 cm) was placed in the femoral artery (percutaneous entry) for rapid blood sampling and physiologic monitoring, as necessary. Additionally, an 18-g teflon catheter was situated in a peripheral vein for bolus i.v. injections, fluid replacement, and supplemental drug administration. The baboon was aligned in the PET imaging device with the use of a plexiglass head holder designed to easily position the animal (*25*). Two studies were carried out with Super PETT IIB, a time-of-flight, 7-slice tomograph with a 50-cm diameter field; and four studies with PETT VI (*26, 27*), a 7-slice tomograph with a 27-cm diameter field.

First, $H_2{}^{15}O$ (30–40 mCi) was injected as a bolus via peripheral vein. The PETT collected a 40-sec image (beginning at the completion of the injection). Timed with the injection, rapid arterial blood samples (every 5 sec) were collected in preweighed 3-ml capped syringes. The blood samples were weighed and counted in a calibrated NaI(Tl) scintillation well detector. The counts in the blood samples, then, are decay-corrected to beginning of PETT collection to provide the necessary input data to determine regional CBF from the $H_2{}^{15}O$ PET images (*28–30*).

After the ^{15}O had decayed, 2–22 mCi of [^{64}Cu]-Cu-PTSM (0.38–4.18 mCi positron equivalents, 2–10 ml) were injected by bolus through the flushed i.v. catheter. With Super PETT IIB, list mode data collection was continuous for 2 hr, after which these data were summed into 1-hr images (0–1 hr, 1–2 hr); as well as sequential 10-min data frames for the duration of the 2-hr collection (0–10 min, 10–20 min, etc.). The ^{64}Cu images obtained with PETT VI were collected as ten 1-min frames (for 20 min maximum).

In two studies, quantitative techniques were utilized to directly evaluate CBF measured with both $H_2{}^{15}O$ and [^{64}Cu]-Cu-PTSM. After the ^{64}Cu injection, rapid arterial blood samples were withdrawn in 3-ml preweighed heparinized (ca. 50 U) syringes. Timed samples (ca. 0.4 ml each) were withdrawn approximately every 5 sec for the first minute, every 10 sec for another minute, then every 30 sec until the end of the image collection. Selected samples were further analyzed; from these a small aliquot (50–100 μl) was quickly added to 1 ml of 95% ethanol and immediately vortexed. All of the samples were weighed and counted as described for $H_2{}^{15}O$ blood-sample analysis. The ethanol extracted samples were centrifuged (15,600 × g for 2 min), the layers separated and counted. Thin-layer chromatography of the ethanol extract was carried out on analytical silica plates eluted with ethyl acetate to determine Cu-PTSM content. The developed plates were scanned on the radiochromatogram analyzer; control samples (heparized blood mixed with [^{64}Cu]-Cu-PTSM in vitro) were extracted with 1 ml of ethanol. After the extraction efficiency was determined by counting the separated layers, a sample of the extract was chromatographed and analyzed.

PET images were quantitatively analyzed with the equation:

$$C_{PET} = m \cdot f \cdot \int_{T_1}^{T_2} \int_{0}^{T} Ca(t) e^{-k(T-t)}\, dt\, dT,$$

which relates the PET-measured tissue activity (C_{PET}) to the single-pass extraction of the tracer (m), local blood flow (f), the start and stop times of the PET scan (T_1 and T_2, respectively), the blood-activity curve [Ca(t)], and the tracer washout rate (k, which is typically estimated by the flow divided by the tissue/blood partition coefficient. With highly extracted tracers, m approaches 1, and, thus, this term can then be ignored (*15,28–33*). With a microsphere analogue, such as Cu-PTSM, the washout rate, k, is negligible and the equation can be rewritten as:

$$C_{PET} = f \int_{T_1}^{T_2} \int_{0}^{T} Ca(t)\, dt\, dT.$$

If scan times T_1 and T_2 are after the point that blood activity, Ca(t), becomes negligible, this equation becomes analogous to standard microsphere techniques (*34,35*).

The acquired images were displayed, and 10–12 regions were assigned to various locations within a single transverse tomographic slice. The method has been previously described (*26–29*). This allows a retrieval of counts within the assigned region dimensions. Qualitative values of counts per minute per pixel from ^{64}Cu-PTSM can be compared to $H_2{}^{15}O$ in the same location. As well, high-blood flow and low-blood regions can be defined, from which ratio data can be generated.

RESULTS AND DISCUSSION

In all cases, the radiolabeled copper complexes were >95% radiochemically pure by TLC and had log p values consistent with those previously reported (*9–11*). With only minor modifications of technique, the synthetic procedure employed will allow the preparation

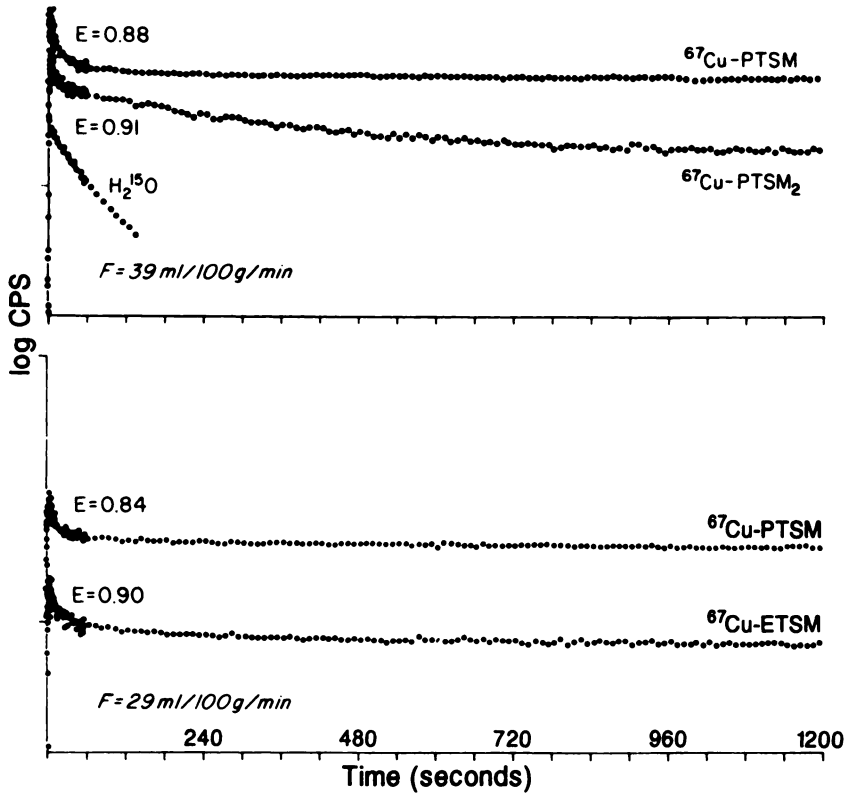

FIGURE 3
Examples of the time-activity curves from a single-pass study following the intracarotid injection of [^{67}Cu]-Cu-PTSM and [^{67}Cu]-Cu-PTSM$_2$. The $H_2{}^{15}O$ data is also graphed from which the CBF (39 mL·min^{-1}·100 g^{-1}) is determined. (Top panel) A comparison of the extraction and clearance of [^{67}Cu]-Cu-PTSM and [^{67}Cu]-Cu-ETSM in a baboon brain following intracarotid bolus injection. (Bottom panel) The Cu-PTSM consistently exhibits microsphere-like retention after 50 sec.

TABLE 1
Baboon Single-Pass Cerebral Extraction Data

Compound	Cerebral blood flow (ml·min^{-1}·100 g^{-1})	Extraction fraction (E)	PS (ml·min^{-1}·100 g^{-1})	E′	(PS)′ (ml·min^{-1}·100 g^{-1})	Primate No.	Experiment No.
Cu-PTSM	36	0.90	83	0.67	39.3	4	7
	38	0.89	83	0.71	47.0	1	2
	42	0.86	83	0.51	31.4	1	4
	44	0.85	85	—	—	1	8
	46	0.83	83	0.64	46.9	1	1
	46	0.73	61	0.53	34.7	2	5
	47	0.87	95	—	—	1	4
	52	0.80	83	0.65	54.6	1	2
	57	0.70	69	0.46	35.1	1	3
	81	0.76	114	0.65	85.0	2	5
	89	0.73	117	0.52	65.3	1	1
Cu-PTSM$_2$	39	0.91	94	—	—	3	6
	41	0.89	90	—	—	3	6
	42	0.91	99	—	—	1	4
	46	0.91	111	—	—	1	4
	74	0.87	152	—	—	1	3
	102	0.69	119	—	—	1	3
Cu-ETSM	38	0.95	114	0.79	59.3	4	7
	41	0.94	115	0.83	72.7	4	7
	44	0.88	93	0.50	30.5	1	8
	45	0.84	81	0.76	64.2	1	6
	47	0.85	90	0.53	35.5	1	8
	63	0.83	112	0.68	71.8	2	5
	76	0.78	114	0.54	59.8	2	5
	88	0.77	128	0.50	60.9	1	3

The E′ (residual fraction) is the fraction of compound retained in the brain over a 5–10-min time period. (PS)′ is the apparent PS value of the retained activity. This will be the apparent in PS value using an imaging time of >5 min.

of copper-labeled Cu-PTSM in less than 5 min, a time frame compatible with the 9.7 min half-life of ^{62}Cu.

The results of our baboon single-pass studies (Table 1 and Fig. 3) are consistent with the previously reported biodistribution results; all three tracers are efficiently extracted into the brain. The time-activity curves obtained with [^{67}Cu]-Cu-PTSM, [^{67}Cu]-Cu-PTSM$_2$, and [^{67}Cu]-Cu-ETSM (Fig. 3) provide examples of the results obtained with lipophilic metal chelates which are extracted in the brain. The PS for Cu-PTSM, Cu-PTSM$_2$, and Cu-ETSM average 87 ± 17 (n = 11), 111 ± 23 (n = 6); and 106 ± 16 (n = 8), respectively (see Table 1).

It was previously reported that [^{67}Cu]-Cu-PTSM affords prolonged microsphere-like retention of radioactivity in the brain (monkey and rat) beyond one minute postinjection (i.v.) (*10*). The brain single-pass extraction studies in the baboon with [^{67}Cu]-Cu-PTSM also demonstrate constant cerebral radioactivity levels after 1 min postinjection (Fig. 3 and Table 1). However, this method (bolus internal carotid injection of tracer with external monitoring of cerebral radiotracer levels) allows accurate determination of tracer cerebral pharmacokinetics in the initial 60 sec following injection, revealing that some clearance of initially extracted tracer from the brain occurs during the first 40–50 sec after injection (Fig. 3). Thus, the tissue trapping of tracer that occurs with Cu-PTSM is not "instantaneous" upon penetration of the BBB, but nevertheless must be a relatively rapid process. When imaging over a time period >2 min, the fraction of activity in the brain is not the fraction extracted but the fraction trapped. We have used the trapped fraction to calculate (PS)′, which is the apparent permeability surface area product obtained when long imaging times (≦ 10 min) are needed. The (PS)′ for the retained Cu-complexes were calculated; (PS)′ for Cu-PTSM was 50.0 ± 18.1 (n = 9) and 53.0 ± 23.2 (n = 8) for Cu-ETSM (Table 1).

Although the more lipophilic Cu-PTSM$_2$ and Cu-ETSM exhibit initial cerebral extraction values greater than that of Cu-PTSM at any given flow, these tracers also show a more prolonged clearance phase. In the case of Cu-PTSM$_2$, tracer slowly clears from the brain over the entire 20 min studied (Fig. 3). This is consistent with the cerebral clearance observed following i.v. injection in a rat model (*10,11*) and can be explained by the known resistance of this complex to reductive decomposition by intracellular sulfhydryl groups (*36–40*). (We presume the apparent trapping of Cu-labeled Cu-PTSM in the brain is the result of the intracellular liberation of ionic copper from the lipophilic chelate complex via this known redox process with cellular thiols.) The Cu-ETSM complex should have a reduction potential comparable to that of Cu-PTSM (*36–39*); however, our studies show that is not trapped in the brain as effectively as Cu-PTSM. This is not entirely unexpected, since the kinetics of the redox reaction with organic thiols and copper(II) bis(thiosemicarbazone) complexes with similar reduction potentials is slowed when sterically bulky substituents are added (*36, 39*). Thus, while the increased lipophilicity that results from addition of a methylene group to the glyoxal sidechain apparently improves tracer extraction into the brain, the benefit is somewhat lost due to a decrease in the efficiency with which the tracer is subsequently trapped. The net result of the increased extraction and more prolonged clearance observed with Cu-ETSM is a (PS)′ value comparable to that of Cu-PTSM.

While none of these copper(II) bis(thiosemicarbazone) complexes penetrate the BBB more efficiently than ^{11}C-butanol or [^{123}I]IMP (*41,42*), they do exhibit higher cerebral extraction than any of the other metal-labeled radiopharmaceuticals that have been proposed as cerebral blood flow agents (e.g., ^{99m}Tc-labeled -d,l-HM-PAO, -ECD, -SQ32097) (*43*).

One disadvantage of the baboon single-pass model is that it provides global not regional values for PS products. It is known that the brain capillary surface area is greater for gray matter than for white matter by a factor of ~3.3 (*24*). If one assumes that the permeability of capillaries in gray and white matter is the same, one can calculate the PS products for gray and white matter and determine the CBF in both of these regions of the brain. For Cu-PTSM, the flow underestimation is less severe in the higher flow gray matter regions of the

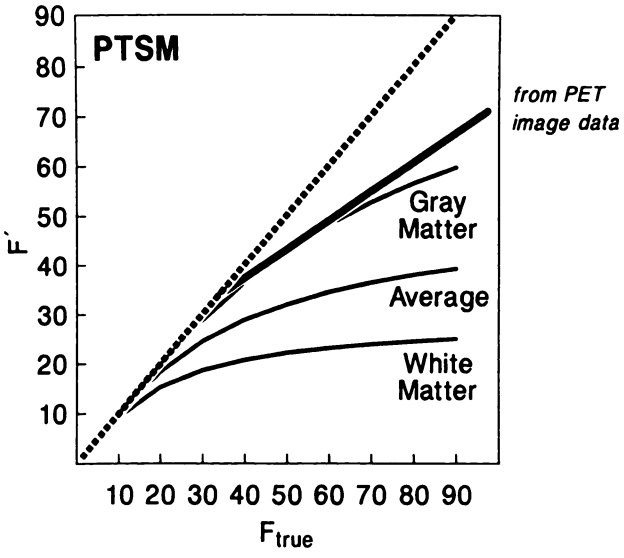

FIGURE 4
Anticipated Cu-PTSM underestimation of blood flow (mL·min^{-1}·100 g^{-1}) in gray and white matter regions of the brain calculated from the measured (PS)′ values determined and assuming gray/white variations result from known differences in capillary surface area (*24*). Also shown is the regression line obtained from analysis of [^{64}Cu]-Cu-PTSM PET image data (vide infra).

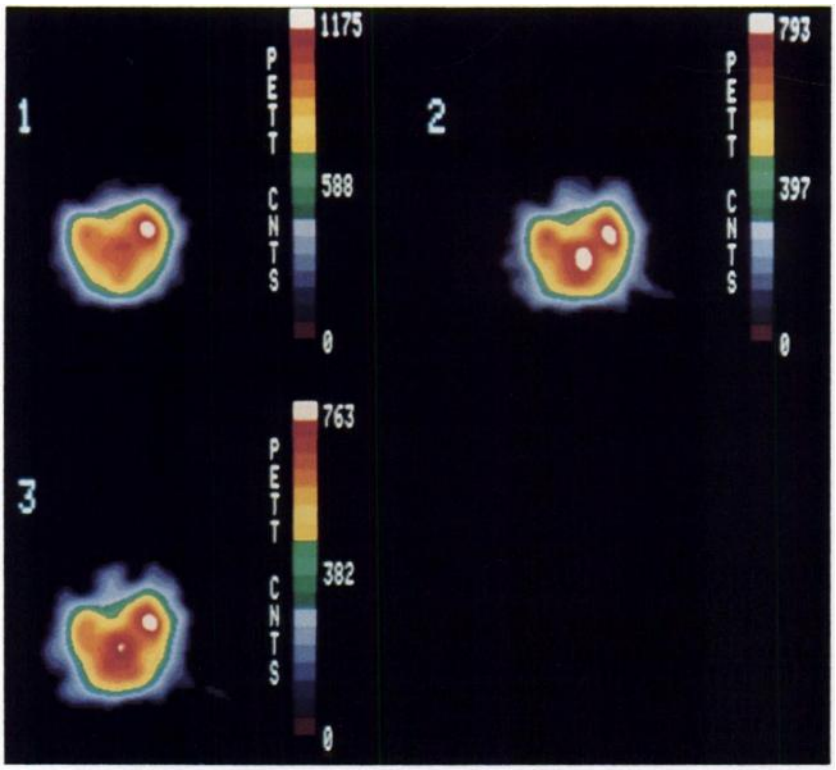

FIGURE 5
A comparison of a 40-sec $H_2{}^{15}O$ image (1) with [^{64}Cu]-Cu-PTSM images obtained 0–1 hr (2) and 1–2 hr (3) after administration of the ^{64}Cu-labeled radiopharmaceutical in PETT IIB. The PET slice shown corresponds approximately to a midbrain transverse section at the level of the occular orbits.

brain than in the lower flow white matter regions of the brain (Fig. 4).

The ultimate goal in designing a radiopharmaceutical to measure blood flow is to be able to obtain images that allow measurement of absolute regional blood flow ($mL \cdot min^{-1} \cdot 100\ g^{-1}$). Figure 5 compares the qualitative distribution of $H_2{}^{15}O$ (40 sec) with [^{64}Cu]-Cu-PTSM imaged for 2 hr (0–1 hr and 1–2 hr frames). The relative ratios of radioactivity in high flow regions compared to radioactivity in low-flow regions are similar for $H_2{}^{15}O$ (2.4) and Cu-PTSM (2.7); this is represented by very similar images obtained with $H_2{}^{15}O$ and [^{64}Cu]-Cu-PTSM (Fig. 5). The counts per minute per pixel from three regions (two high-flow and one low-flow) in the Cu image were determined. The time-activity plots show that the ^{64}Cu distribution does not change over the 2-hr time period (Fig. 6). Additionally, these data suggest that the lack of washout or redistribution of Cu-PTSM over the 2-hr period is not flow-dependent.

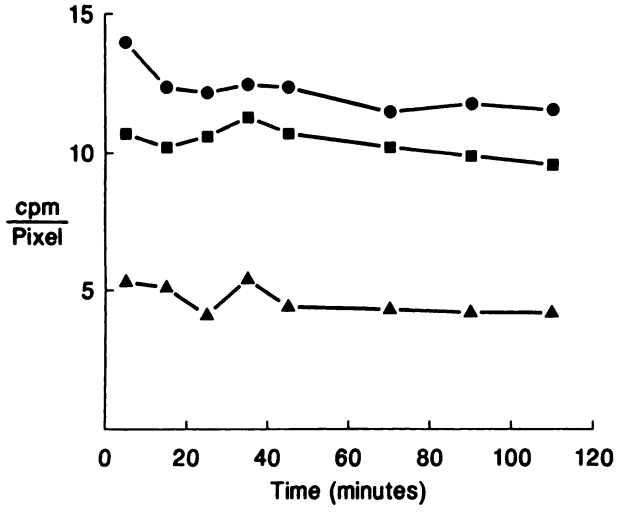

FIGURE 6
An example from one study of the Cu-PTSM radioactivity in three brain regions (cpm/pixel) as a function of time, demonstrating that there is very little washout or redistribution of copper radioactivity in either high or low blood flow areas during the 2-hr study.

In order to quantitate rCBF, the true arterial input function is required. A comparison of the counts per milliliter per second in the blood with the counts corrected for Cu-PTSM metabolism is shown in Figure 7. After ~1 min, all of the radioactivity in the blood is due to metabolites. The TLC migration pattern of the blood extracts show that none of the blood activity is present as the lipophilic Cu-PTSM complex beyond 2 min postinjection (Fig. 7). Both the single-pass and PET studies reveal constant brain levels of ^{67}Cu or ^{64}Cu beyond 1 minute after the radiolabeled Cu-PTSM injection, making it exceedingly unlikely that the radioactive metabolites of Cu-PTSM significantly penetrate the BBB. The inability of the Cu-labeled Cu-PTSM metabolite(s) in the blood to penetrate the BBB has been directly demonstrated in rats. When a blood sample is obtained 5 min following i.v. [^{67}Cu]-Cu-PTSM administration to a rat and an aliquot of that blood promptly injected into a second rat, the brain levels of ^{67}Cu in the second rat do not exceed that which can be

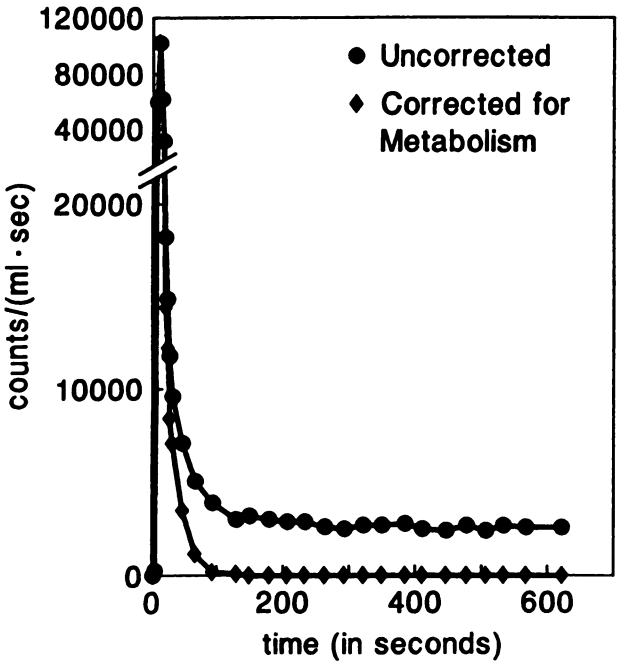

FIGURE 7
Counts per second per ml of arterial blood sampled at time intervals after the i.v. bolus injection of [^{64}Cu]-Cu-PTSM were used to obtain a time-activity curve (●). The curve was corrected (◆) to account for circulating radioactivity that was not Cu-PTSM, determined by TLC.

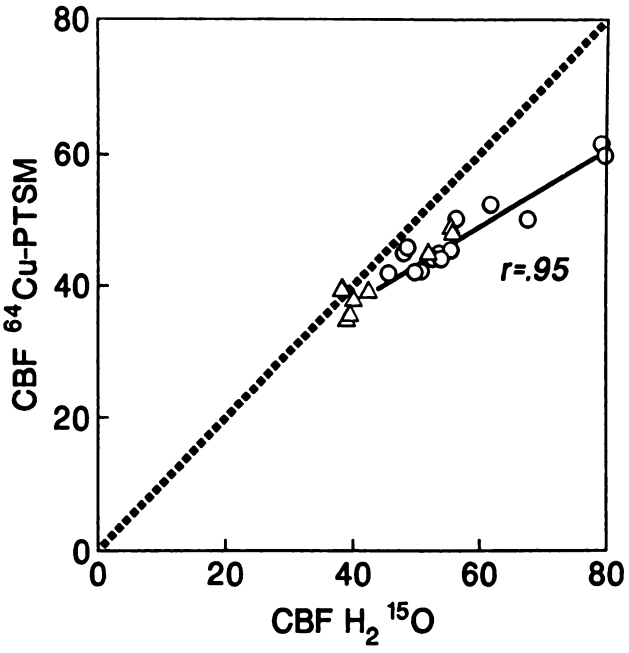

FIGURE 9
A comparison of quantitative rCBF (mL·min·100 g^{-1}) determined with $H_2{}^{15}O$ and [^{64}Cu]-Cu-PTSM in various regions of the brains of two baboons from two experiments in PET VI (○ = experiment 1, n = 4; △ = experiment 2, n = 9). The solid line was determined by linear regression analysis (n = 23). The dashed line is the line of identity.

attributed to blood radioactivity (Green MA, unpublished results).

The true input function was utilized to calculate rCBF using the microsphere model described. This was done on a region-by-region basis; the region selection was as indicated in Figure 8. The [^{64}Cu]-Cu-PTSM image, from 1–10 min postinjection, was utilized for the CBF quantification. The $H_2{}^{15}O$ blood flow was determined as previously described (*31*). The quantitative values obtained with $H_2{}^{15}O$ and Cu-PTSM for CBF in 23 brain regions for two primates are compared in Figure 9. At relatively high flows (>40 ml·min^{-1}·100 g^{-1}), the Cu-PTSM does underestimate CBF as calculated from the PS of Cu-PTSM (determined in the single-pass model). In fact, the regression line from the flow values determined with PET (Fig. 9) overlie the calculated curve for the anticipated flow values in gray matter of the brain (Fig. 4). This might have been anticipated since regions of relatively high blood flow (>40 ml·min^{-1}·100 g^{-1}) were selected from the PET image data (see Fig. 9).

In conclusion, Cu-PTSM is a new radiopharmaceutical that can be labeled with generator-produced ^{62}Cu and has the potential for the qualitative and quantitative assessment of rCBF in the brain. This agent also will allow repeated blood flow studies to be carried out in PET centers without a cyclotron. [^{62}Cu]-Cu-PTSM

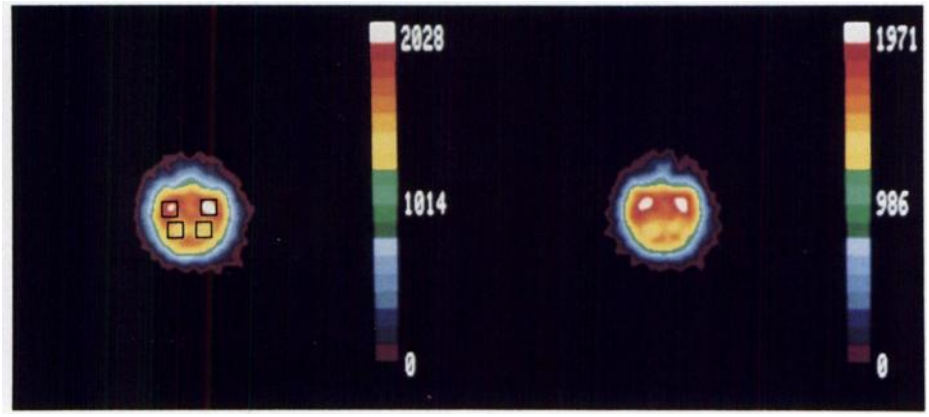

FIGURE 8
A comparison of a [^{64}Cu]-Cu-PTSM 60–600-sec PET scan (left) with a 40-sec $H_2{}^{15}O$ scan (right). Regions of interest were defined (approximate region size shown on left) in order to quantitate regional cerebral blood flow measured by each of the two tracers.

should allow quantification of rCBF with the use of all commercially available tomographs. As addressed by Herscovitch (*44*), the quantitative PET/autoradiographic method using $H_2{}^{15}O$ is only applicable with scanners that operate accurately at a very high count rate. The steady-state approach utilizing inhaled CO_2 (*45*) or i.v. administration of $H_2{}^{15}O$ (*46*) is applicable with all tomographs, but suffers from the fact that measurement errors of tissue radioactivity produce proportionally larger errors in flow measurements (*44*). The Cu-PTSM technique, which could be repeated approximately every 20 min, has advantages over the steady-state technique, which can also only be repeated approximately every 20 min.

ACKNOWLEDGMENTS

This work was supported by DOE grant DE-FG02-87ER60512, grants NS06833, HL13851, and HL01801 from the National Institutes of Health, and grant CA46909 from the Reactor Sharing Program at the University of Missouri Research Reactor.

The authors greatly appreciate the technical assistance of David Perry and John Hood, Jr., and the helpful discussions with Dr. Joel S. Perlmutter.

REFERENCES

1. Lederer CM, Shirley VS, eds. *Table of Isotopes.* 7th Edition. New York: John Wiley & Sons; 1978.
2. Moody DC, Peterson EJ, eds. *Proceedings of the DOE workshop on the role of a high-current accelerator in the future of Nuclear Medicine.* Springfield, VA: National Technical Information Service; 1989.
3. Knapp FF, Jr., Butler TA, eds. *Radionuclide generators: new systems for nuclear medicine applications.* Washington, DC: Am Chem Soc; 1984.
4. Robinson GD, Zielinski FW, Lee AW. Zn-62/Cu-62 generator: a convenient source of copper-62 radiopharmaceuticals. *Int J Appl Radiat Isot* 1980; 31:111–116.
5. Ueda N, Nakamato S, Tanaka Y, et al. Production of Zn-62 and development of Zn-62/Cu-62 generator systems [Abstract]. *J Nucl Med* 1983; 24:P124.
6. Yagi M, Kondo K. A Cu-62 generator. *Int J Appl Radiat Isot* 1979; 30:569–570.
7. Robinson GD. Cyclotron-related radiopharmaceutical development program at UCLA. *Prog Nucl Med* 1978; 4:80–92.
8. Suzuki K, Iwata R. A multi-target assembly in an irradiation with high energy particles. Simultaneous production of ^{123}I, ^{62}Zn and $^{13}NH_3$. *Int J Appl Radiat Isot* 1977; 28:663–665.
9. Green MA. A potential copper radiopharmaceutical for imaging the heart and brain: copper-labeled pyruvaldehyde bis(N^4-methylthiosemicarbazone). *Nucl Med Biol Int J Radiat Appl Instrum*, Part B 1987; 14:59–61.
10. Green MA, Klippenstein DL, Tennison JR. Copper(II) bis(thiosemicarbazone) complexes as potential tracers for evaluation of cerebral and myocardial blood flow with PET. *J Nucl Med* 1988; 29:1549–1557.
11. Green MA, John E. Structure-activity relationships for potential metal-labeled blood flow agents: comparison of copper(II) bis(thiosemicarbazone) derivatives. *J Lab Cmpds Radiopharm* 1989; 26:351–353.
12. Raichle ME, Eichling JO, Grubb RL. Brain permeability of water. *Arch Neurol* 1974; 30:319–321.
13. Raichle ME, Grubb RL, Eichling JO, Ter-Pogossian MM. Measurement of brain oxygen utilization with radioactive oxygen-15: experimental verification. *J Appl Phys* 1976; 40:638–640.
14. Grubb RL, Raichle ME, Eichling JO, Ter-Pogossian M. The effects of changes in $paCO_2$ on cerebral blood volume, blood flow, and vascular mean transit time. *Stroke* 1974; 5:630–639.
15. Raichle ME, Larson KB. The significance of the NH_3-NH^+_4 equilibrium on the passage of ^{13}N-ammonia from blood to brain. *Circ Res* 1981; 48:913–937.
16. *Handbook on nuclear activation cross-sections. Neutron, Photon and charged-particle nuclear reaction cross-section data.* Technical reports series No. 156. Vienna: International Atomic Energy Agency; 1974:774.
17. Dyer FF, Leddicotte GW. *The radiochemistry of copper.* Washington DC: National Academy of Sciences/National Research Council; Publication NAS-NS 3027; 1961.
18. Hetherington EL, Sorby PS, Camakaris J. The preparation of high specific activity copper-64 for medical diagnosis. *Appl Radiat Isot* 1986; 37:1242–1243.
19. Welch MJ, Lifton JF, Ter-Pogossian MM. The preparation of millicurie quantities of oxygen-15 labeled water. *J Labeled Cmpds* 1969; 5:168.
20. Ter-Pogossian, Eichling JO, Davis DO, Welch MJ, Metzger JM. The determination of regional cerebral blood flow by means of water labeled with radioactive oxygen-15. *Radiology* 1969; 93:31–40.
21. Eichling JO, Raichle ME, Grubb RL, Jr, Ter-Pogossian MM. Evidence of the limitations of water as a freely diffusible tracer in brain. *Circ Res* 1974; 35:358.
22. Raichle ME, Hartman BK, Eichling JO, Sharpe LG. Central noradrenergic regulation of cerebral blood flow and vascular permeability. *Proc Nat Acad Sci* 1975; 72:3726.
23. Crone C. The permeability of capillaries in various organs as determined by use of the 'indicator diffusion' method. *Acta Physiol Scand* 1963; 58:292–305.
24. Raichle ME, Eichling JO, Straatmann MG, Welch MJ, Ter-Pogossian MM. Blood brain barrier permeability of ^{11}C-labeled alcohols and ^{15}O-labeled water. *Am J Physiol* 1976; 230:543–552.
25. Perlmutter JS, Kilbourn MR, Welch MJ, Raichle ME. Non-steady-state measurement of in vivo receptor binding with positron emission tomography: "dose-response" analysis. *J Neurosci* 1989; 9:2344–2352.
26. Ter-Pogossian MM, Ficke DC, Hood JT, Yamamato M, Mullani NA. PETT-VI: a positron emission tomograph utilizing cesium fluoride scintillation detectors. *J Comput Assist Tomogr* 1982; 6:125–133.
27. Yamamato MM, Ficke DC, Ter-Pogossian MM. Performance study of PETT VI: a positron computed tomograph with 288 cesium fluoride detectors. *IEEE Trans Nucl Sci* 1982; 29:529–533.
28. Herscovitch P, Markham J, Raichle ME. Brain blood flow measured with intravenous $H_2{}^{15}O$. I. Theory and error analyses. *J Nucl Med* 1983; 24:782–789.
29. Raichle ME, Martin WRW, Herscovitch P, Mintun MA, Markham J. Brain blood flow measured with intravenous $H_2{}^{15}O$. II. Implementation and validation. *J Nucl Med* 1983; 24:790–798.
30. Mintun MA, Raichle ME, Martin WRW, Herscovitch P. Brain oxygen utilization measured with O-15 radiotracers and positron emission tomography. *J Nucl Med* 1984; 25:177–187.
31. Herscovitch P, Raichle ME, Kilbourn MR, Welch MJ. Positron emission tomographic measurement of cerebral blood

flow and permeability-surface area product of water using [^{15}O]water and [^{11}C]butanol. *J Cereb Blood Flow Metab* 1987; 7:527–542.
32. Kety SS. Theory of blood-tissue exchange and its application to measurement of blood flow. *Methods Med Res* 1960; 8:223–227.
33. Larson KB, Markham J, Raichle ME. Comparison of distributed and compartmental models for analyses of cerebral blood flow measurements. *J Cereb Blood Flow Metab* 1985; 5(suppl 1):5649–5650.
34. Foun-Chung F, Schuessler GB, Chen RYZ, Chen S. Determinations of blood flow and shunting of 9- and 15-μm spheres in regional beds. *Am J Physiol* 1979; 237:H25–H33.
35. Heymann MA, Payne BD, Hoffman JIE, Rudolph AM. Blood flow measurements with radionuclide-labeled particles. *Prog Cardiovasc Dis* 1977; 20:55–79.
36. Winkelmann DA, Bermke Y, Petering DH. Comparative properties of the antineoplastic agent, 3-ethoxy-2-oxobutyraldehyde bis(thiosemicarbazonato) copper(II) and related chelates: linear free energy correlations. *Bioinorg Chem* 1974; 3:261–277.
37. Petering DH. Physicochemical properties of the antitumor agent, 3-ethoxy-2-oxobutyraldehyde bis(thiosemicarbazonato) copper(II). *Bioinorg Chem* 1972; 1:255–271.
38. Petering DH. The reaction of 3-ethoxy-2-oxobutyraldehyde bis(thiosemicarbazonato) copper(II) with thiols. *Bioinorg Chem* 1972; 1:273–288.
39. Petering DH. Carcinostatic copper complexes. In: Sigel H, ed. *Metal ions in biological systems. Vol 11.* New York: Marcel Dekker; 1980:197–229.
40. Minkel DT, Saryan LA, Petering DH. Structure-function correlation in the reaction of bis(thiosemicarbazonato) copper(II) complexes with Ehrlich ascites tumor cells. *Cancer Res* 1978; 38:124–129.
41. Dischino DD, Welch MJ, Kilbourn MR, Raichle ME. Relationship between lipophilicity and brain extraction of C-11-labeled radiopharmaceuticals. *J Nucl Med* 1983; 24:1030–1038.
42. Winchell HS, Horst WD, Braun L, Oldendorf WH, Hattner R, Parker H. N-Isopropyl-[^{123}I]p-Iodoamphetamine: single-pass brain uptake and washout; binding to brain synaptosomes; and localization in dog and monkey brain. *J Nucl Med* 1980; 21:947–952.
43. Mathias CJ, Welch MJ, Lich L, Raichle ME, Volkert WA, Hung JC. Single-pass extraction of d,l and meso Tc-99m HM-PAO in primate brain [Abstract]. *J Nucl Med* 1988; 29:747–748.
44. Herscovitch P. Measurement of regional cerebral hemodynamic and metabolism by positron emission tomography. In: Boulton AA, Baker GB, Boisvert DPJ, eds. *Neuromethods, imaging and correlative physicochemical techniques.* Clifton, New Jersey: Humana Press; 1988:179–232.
45. Frackowiak RSJ, Lenzi GL, Jones T, Heather JD. Quantitative measurement of regional cerebral blood flow and oxygen metabolism in man using ^{15}O and positron emission tomography: theory, procedure and normal values. *J Comput Assist Tomogr* 1980; 4:727–736.
46. Jones SC, Greenberg JH, Dann R, et al. Cerebral blood flow with the continuous infusion of oxygen-15 labeled water. *J Cereb Blood Flow Metab* 1985; 5:566–575.